

## Abstract

In recent years, organizations have explored various methods of quantifying soil carbon to document carbon flux or provide economic incentive to farmers utilizing management practices that sequester carbon in their soil. This study utilizes soil samples from three livestock farms in Rockbridge County, Virginia practicing either conventional or regenerative agricultural practices. Two adjacent farms graze carbonate residual soils and the third farm is on alluvial soils. We chose sampling locations using conditioned Latin Hypercube Sampling (cLHS) to replicate the distribution of soil, topographic, and remote sensing covariates in the feature space of the sampled points. These topographic and remote sensing variables represent our understanding of soil development and carbon sequestration at the field scale using widely available data. Applied covariates include management practice, seasonal maximum NDVI from Planet imagery, USDA gSSURGO soil series clay content, plus slope, aspect, and Saga Wetness Index from LIDAR-based 3-m-DEMs. Sampling density was minimized until distributions of the covariate input dataset diverged from those of the sampled points, as measured by the value of the cLHS objective function. At each selected sample point, we measured total carbon in a combustion elemental analyzer and inorganic carbon with a pressure calcimeter. Random forest (RF) models were able to predict SOC stocks more accurately with  $R^2$  values of  $0.59 \pm 0.04$  and  $0.22 \pm 0.03$  at the Alluvial Site and Management Comparison sites, respectively. The multivariate linear model (LM) has  $R^2$  values of  $0.50 \pm 0.06$  and  $0.12 \pm 0.01$  at the Alluvial Site and Management Comparison sites, respectively. Both models seem unable to produce accurate predictions of SOC stocks at the point scale, but all models produce an estimate of the mean SOC stocks of the site to within  $1 \text{ Mg C ha}^{-1}$ .

## **Introduction**

Measuring soil organic carbon (SOC) is necessary in soil carbon sequestration, because it allows for the implementation of a carbon credit system directed towards rewarding individuals for adopting practices that sequester carbon in the soil. According to Follett and Reed (2010), “Virtually every major economic analysis of how the US can begin to slow, stop, and reverse its growing emissions of GHG relies upon soil C sinks as a near-term, low-cost pool of reductions to atmospheric GHG emissions.” However, there is a major roadblock to implementing soil carbon credits: the prohibitive cost of performing the soil sampling required to accurately measure SOC. An Australian study focusing on measuring SOC in cropland found that it costs an estimated AU\$2,500 (approximately USD\$2,500 +/- \$100 at the time) to accurately measure SOC across a 168 ac plot using soil cores and an elemental analyzer (Singh et al., 2013).

Implementation of a soil carbon credit system will be difficult under these standards because it is likely that the cost of performing the sampling will outweigh the economic benefit provided by the carbon credits. It follows logically that a more cost effective method of measuring SOC is required to expand the feasibility of soil carbon credits.

Digital soil mapping offers the opportunity to explore a technological way to reduce costs for SOC sampling. Digital soil mapping “can be defined as the creation and population of spatial soil information systems by numerical models inferring the spatial and temporal variations of soil types and soil properties from soil observation and knowledge and from related environmental variables” (Lagacherie, 2008). This technique surged in popularity following the publishing of a landmark review paper that detailed a generalizable framework for mapping soil classes or properties using a GIS, field sampling and laboratory analysis, and numerical modeling (McBratney et al., 2003). Digital soil mapping has since been used rigorously to

predict SOC at the field scale (e.g. Guo et al., 2020; Kane et al., 2019; Lacoste et al., 2014; Malone et al., 2009; Pouladi et al., 2019; Zhang et al., 2020). Environmental covariates used in these studies include elevation, slope, curvature, topographic wetness, valley bottom/ridge top flatness, bedrock lithology, cosine of aspect, sine of aspect, slope length, normalized difference vegetation index (NDVI), spectral bands, among others. Numerical and machine learning methods employed in these studies include Cubist, Random Forest, kriging, stepwise regression, partial least square regression, backpropagation neural networks, extreme learning machine, support vector machine, Bayesian additive regression tree, and generalized linear model, among others. These studies have predicted OC content of soils with  $R^2$  values ranging from 0.1-0.91, indicating that the efficacy of these models varies greatly dependent on soil sampling methodology, study area, and choices throughout the modelling process (Pouladi et al., 2019; Malone et al., 2009). In this study we aim to examine the validity of measuring and predicting pasture-scale variability and SOC stocks in Rockbridge County, Virginia using cLHS, multivariate linear models (LM), and Random Forest models (RF).

## **Study Areas**

### **Management Comparison Site**

Two study areas are located on adjacent pastures in Raphine, Virginia. These study areas consist of Verdant Acres, a rotationally grazed farm with approximately 30 acres of pasture, and an adjacent, 110 acre set of conventionally managed pastures to the east and southeast. Both of these sites are underlain by the Cambrian Elbrook formation, which is fine-to medium-grained, thinly bedded limestone and dolostone (Wilkes et al., 2007). These pastures include floodplain along Moffets Creek and gradually sloping hills that converge to the floodplain from the

northeast/southwest (Fig. 1). Floodplain soils are part of the Buckton-Weaver complex, composed of silt loam and fine sandy loam at slopes of 0-3%. The soils of the surrounding upper slopes are part of the Frederick-Caneyville complex and Frederick silt loam, which are composed of silt loam to silty clay loam. The primary distinction between these two units is that the Frederick-Caneyville complex is significantly rockier than the Frederick silt loam (Web Soil Survey, 2019).

Before fall of 2018, Verdant Acres was part of the adjacent parcel and was continuously stocked with cattle. Following late 2018, management practices changed to rotationally grazed sheep and goats, followed by laying hens during most of the year. Sheep and goats are moved to a new paddock every few days in the summer, and chickens follow about two days behind. Broiler chickens are also moved throughout the pastures by way of a movable chicken coup primarily used for spot fertilization.

### **Alluvial Site**

Our third study area is located in Kerrs Creek Virginia, and contains approximately 65 acres of pastures that have been rotationally grazed by sheep, cattle, pigs, and chickens from 2016-present. Prior to 2016, these pastures were continuously stocked with cattle and intermittently hayed. This 65-acre site is a terrace and floodplain of Kerrs Creek underlain by the Ordovician Edinburg limestone, which is responsible for the sinkholes in the terrace pastures and consists of “a fine-grained, dense, black, thinly-bedded limestone interlayered with buff-weathering, fissile, black shale” (Wilkes et al., 2007). The terrace hosts 6 sinkholes that are obvious on a slope map of the farm (Fig. 1). Soils along the floodplain are part of the Ingledove loam, consisting of loam and clay loam. The terrace tread and scarp and the majority of soils to the north and east of it are part of the Shottower fine sandy loam of varying slopes. This unit is

made up of fine sandy loam, clay loam, clay, and gravelly clay. Soils in a small portion of the northwestern corner of the study area are part of the Tygart-Purdy complex, which is made up of silt loam, silty clay, and clay (Web Soil Survey, 2019).

## **Methodology**

### **Conditioned Latin Hypercube Sample Location Selection**

I chose field sampling locations using a conditioned Latin Hypercube Sampling procedure (cLHS) derived from Minasney and McBratney (2006). I choose this sampling procedure in order to replicate the feature space of the field sites in our selected sampling locations using widely available geospatial data. The covariates that I inputted into the cLHS program are aspect, a topographic wetness index derived using the SAGA Wetness Index (SWI), soil map unit clay content, agricultural management type, and a maximum value composite of normalized difference vegetation index (NDVI MVC) values taken over a growing season. I chose these covariates in order to best fulfill the scorpan-SSPFe framework put forth by McBratney et al. (2003) using data that is widely available and easily accessible.

The data sources for these layers were a 1m LIDAR DEM, Planet satellite imagery data taken from March to November of 2019, and the USDA Gridded Soil Survey Geographic Database (Virginia Department of Mines, Minerals, and Energy, 2020; Soil Survey Staff, 2019; Planet Team, 2020). Before running analyses, I uniformized all data layers to the same coordinate system, cell size, and extent. Additionally, I drained several sinks in the DEMs in areas where it was necessary. I then exported the uniformized layers as Esri shapefiles for use in the cLHS R package, which is based on Minasney and McBratney (2006).

A Planet satellite image was selected each week from March through November of 2019 in order to represent the entire growing season. At the Management Comparison Site there were five weeks when no suitable images were available due to cloud cover, and at the Alluvial Site there were three weeks when there was no suitable imagery due to cloud cover. 39 images were selected for the Alluvial Site and 37 images were selected for the Management Comparison Site. A normalized difference vegetation index (NDVI) was then calculated for each image before the corresponding images for each site were merged into a maximum value composite (MVC) image using the SAGA Mosaic Raster Layers function.

### **Field Sampling**

Coordinate points selected by the cLHS procedure were loaded into a Trimble GeoExplorer GeoXH 6000 GPS in preparation for field sampling. Upon arriving at each sampling point I placed the GPS on the ground, stood with the GPS between my feet, and dropped a small flag over my shoulder to add an element of randomness to the exact sampling point. I then drove a 1/8 in. steel rod into the ground adjacent to the flag in order to check for bedrock or large clasts in the immediate subsurface. If the rod met an obstacle at a shallow depth, then I removed the rod and drove it in at four perpendicular points each 20 cm from the location of the flag. If all the locations were shallow, then I took the soil core at the flag's location. If a longer core was available at one of the perpendicular points, then I took the soil core at the point that allowed us the longest core.

I then placed a 2.5 cm diameter slide hammer corer directly adjacent to the driving rod, being sure to clear any vegetation from the mouth of the corer without disturbing the surface horizon. Once the corer tip was firmly on the soil surface, we drove it to the depth of resistance or to completion depth (approximately 35 cm). We placed the GPS receiver against the barrel of

the soil corer and recorded a point to cross reference against the initial cLHS points. We also measured the distance from the surface to a predetermined height on the soil corer to estimate the length of the soil core and constrain compaction during coring.

We extracted the corer from the soil by hand, or using a fence post puller for particularly stubborn samples. We then pushed the soil core out of the barrel of the corer into a PVC trough, in the correct orientation, using a wooden dowel. At this point we recorded the actual length of the core, photographed it, and split the core into sections based on visible pedological features. In the case of particularly uniform cores, we split the core into equal sections to capture assumed variation within the core.

### **Sample Preparation**

Upon returning to the lab, I opened each of the individual sample bags and left them to air dry for several weeks. Once the samples had thoroughly dried I weighed each sample, gently crushed them, sieved them to 2 mm, and weighed them once more to derive air dry bulk density for each soil subsample. I weighed all the material that was sieved out and placed it into its own bag for completeness. After noting the weight of each soil sample, they were placed in a drying oven at 105°C for 8 hours. I then split each sample into two portions, one to be used for total and inorganic carbon analysis and one for future analyses.

### **Elemental Analyzer for Total Carbon**

I derived total carbon (TC) content for each soil sample using a CN elemental analyzer. I loaded 15 mg +/- 0.2 mg of each soil sample into a tin cup, noted the weight of each sample, and loaded them into a tray that also contained 0.5 mg and 1.0 mg Acetanilide standards, blanks, and soil bypasses spread throughout each run. The elemental analyzer software I utilized for this process used the response of these Acetanilide standards to construct a linear regression which

was used to derive the TC and nitrogen content for each sample. Error for TC content was estimated based on variance ( $1\sigma$ ) of TC content of Acetanilide standards. This variance was converted to a percentage, combined with the variance estimated from the pressure calcimeter method, and applied to SOC stocks.

### **Pressure Calcimeter for Inorganic Carbon**

I derived inorganic carbon (IC) content for each of the soil samples using the pressure calcimeter method discussed in Fannesbeck et al. I initially ran 10 grams of each soil sample, and any samples that either reached the amperage limit of the pressure calcimeter or explosively released their pressure were then rerun using two grams of soil. Using the  $\text{CaCO}_3$  calibration curve generated with each sample run, I calculated a %IC for each soil sample. Error for IC content was estimated based on maximum variance observed among triplicate samples included in each run. Variance was generally low among triplicate samples, but one sample had a particularly high variance (ie. difference of 19.6%). I then calculated OC for each soil sample by subtracting this IC value from the TC value derived from the elemental analyzer. As mentioned above, the estimated variance for IC was combined with the variance estimated for TC to derive a total variance of 21.2%. This value was then applied to SOC stocks.

### **Statistical Modelling**

A RF and LM were constructed for both the management comparison and alluvial site using the randomForest and caret packages in RStudio, respectively. Covariates used for these models included slope, northness, eastness, elevation, soil unit clay content, and SWI for both sites with the addition of management type for the management comparison type. The efficacy of each model was then examined by iteratively conducting repeated K-fold cross validation to obtain a  $R^2$  value and associated error.



## **Results**

### **Total Organic Carbon Stocks**

Average soil organic carbon expressed in areal units (Mg/ha) to 25 cm depth shows little variation among the pasture study sites (Fig. 2).

A t-test of these groups shows no significant difference between them ( $\alpha = 0.05$ ).

Although not statistically different, the Alluvial Site has the lowest carbons stocks, and between the conventional and regenerative comparison sites, the conventional site has somewhat higher SOC stocks.

### **Spatial Variation in SOC at Depth**

SOC percentage decreases logarithmically with depth (Fig. 3) at both sites. At the Alluvial Site these mean depth fractions form clear groups at 5 cm, 15 cm, and 27 cm and have SOC contents between 2-5%, 1-2%, and 0.5-2%, respectively. At the Management Comparison Site these mean depth fractions form groups at 4 cm, 15 cm, and 27 cm and have SOC contents between 2-8%, 1-5%, and 0.5-2.5%, respectively. The uppermost section likely corresponds to the dark, organic horizon. At intermediate depths the samples follow the same smooth, logarithmic pattern. The Management Comparison site has several outliers, particularly in the uppermost fraction. Of note is that both of the largest outliers are the samples in which SOC content was extrapolated downwards based on the bulk density of the nearest spatial point.

### **SOC Stocks by Geomorphic Landforms**

Average SOC stocks at the Alluvial Site vary with geomorphic position (Fig. 1, Fig. 3). Landforms from greatest to least average SOC stocks to 25 cm ( $\text{Mg C ha}^{-1} \pm$  estimated error)

are the floodplain ( $50.1 \pm 10.6$ ), terrace ( $42.2 \pm 8.9$ ), scarp ( $37.4 \pm 7.9$ ), and upper slope ( $34.1 \pm 7.2$ ) (Fig. 3).

The relationship between average SOC stocks and geomorphic position at the Management Comparison Site is less distinct than at the Alluvial Site. Landforms from greatest to least average SOC stocks to 25 cm ( $\text{Mg C ha}^{-1} \pm \text{standard error}$ ) are the upper slope ( $58.5 \pm 12.4$ ), floodplain ( $53.3 \pm 11.3$ ), and terrace ( $48.4 \pm 10.3$ ) (Fig. 3).

### **Modelling Results**

Individual predictors at the Management Comparison Site display weaker linear relationships in comparison to those at the Alluvial Site (Figs. 4 and 5). At both sites, RF performs better than the LM at predicting SOC stocks with an  $R^2 \pm \text{standard error}$  of  $0.59 \pm 0.04$  and  $0.22 \pm 0.03$  at the Alluvial Site and Management Comparison Site, respectively. The  $R^2 \pm \text{standard error}$  of SOC stocks predicted by the LM are  $0.50 \pm 0.06$  and  $0.12 \pm 0.01$  at the Alluvial Site and Management Comparison Site, respectively (Figs. 6 and 7). The mean values of  $\text{Mg SOC ha}^{-1} \pm \text{estimated error}$  for each model can be found in Table 2.

At the Alluvial Site, NDVI MVC, soil map unit clay content, SWI, northness, and eastness all have a positive relationship with SOC stocks whereas slope has a negative relationship (Fig. 4). At the Management Comparison Site, regenerative and conventional treatments display the opposite relationship between NDVI MVC and SOC stocks. NDVI MVC has a positive relationship with SOC stocks at the Regenerative Management Comparison Site and a negative relationship with SOC Stocks at the Conventional Management Comparison Site. The strongest relationships between covariates and SOC stocks at the Management Comparison Site are NDVI MVC ( $R^2 = 0.25$ ), SWI ( $R^2 = 0.15$ ), and northness ( $R^2 = 0.09$ ), all at the

Regenerative Management Comparison Site (Fig. 5 and Table 1). All other relationships displayed at the Management Comparison Site have an  $R^2 < 0.02$ .

Interpolated maps of residuals for both RF and LM models display a marked similarity in the spatial error for each model (Fig. 8). At the Alluvial Site, the largest positive residuals are concentrated in the upper slope to the northeast and the largest negative residuals are concentrated in two regions oriented north to south - one that divides the floodplain and terrace in the southwestern portion of the study site and another that is juxtaposed between the upper slope and terrace in the northernmost portion of the study site. Neither over- or under-predictions are obviously tied to any covariate or geomorphic unit.

The Management Comparison Site has larger residuals compared to the Alluvial Site. The largest positive residuals at the Management Comparison Site are concentrated in the southwestern portion of the floodplain and an area that contains portions of the terrace and upper slope in the southeast of the study site. The largest negative residuals at the Management Comparison Site are concentrated in the northeastern portion of the floodplain and in the upper slope in the eastern portion of the study site.

## **Discussion**

Observed SOC stocks to 25 cm at the Alluvial Site and Management Comparison Site are comparable to those reported for both regenerative and continuously stocked pastures in the southeastern United States (Franzluebbbers, 2010; Mosier et al., 2021; Yang et al., 2020). Our observed SOC stocks to 25 cm are similar to those reported by Mosier et al. and near the maximum values reported by Yang et al. and Franzluebbbers et al. Most of the carbon is in the upper 10-15 cm, SOC content at depth can be predicted with a  $R^2$  of 0.66-0.82 depending on

sampling site and landform. The Alluvial Site has a stronger relationship between SOC content and depth than the Management Comparison Site with  $R^2 = 0.77$  and  $R^2 = 0.67$ , respectively.

The efficacy of the RF and LM followed a similar trend, with  $R^2 = 0.50-0.59$  at the Alluvial Site and  $R^2 = 0.12-0.22$  at the Management Comparison Site. One possible explanation for the comparatively low predictive power of the models trained at the Management Comparison Site is the inclusion of different management practices into one model. Management practice poorly predicts sample SOC in modelling ( $R^2 = 0.005$ ). This lack of predictive power could mean that any relationship between management practices and SOC stocks wasn't captured in our sampling points, management practices is not a strong predictor for SOC stocks at this site, or that the relationship between SOC stocks and management practices has not had time to develop at the Management Comparison Site given that regenerative practices are only into their 3rd year.

Contemporary literature has reported that regenerative management practices produce anywhere from no significant change to as much as a  $2 \text{ Mg C ha}^{-1} \text{ yr}^{-1}$  increase in SOC stocks compared to conventionally stocked pastures (Chan et al., 2010; Conant et al., 2017; Mosier et al., 2021; Rowntree et al., 2020; Sanderman et al., 2015). Several studies have also documented a slight negative impact of regenerative management practices on SOC stocks (Allen et al., 2014; Conant et al., 2003). Taken together, all these studies have attributed the uncertain relationship between management practices and SOC stocks to a variety of factors including the time since management practices were changed, difficulties involved in selecting "paired" conventionally and regeneratively managed sites, variation of stocking intensity, frequency, and duration between various management practices, and other factors (Allen et al., 2014; Chan et al., 2010; Conant et al., 2017; Conant et al., 2003; Mosier et al., 2021; Sanderman et al., 2015). Additional research is

needed to further quantify the effect of changes in grazing management practices and SOC stocks.

Moving on from causal to procedural sources of error, much of the error estimated in calculating SOC stocks originated during the pressure calcimeter procedure used to derive IC content (the pressure calcimeter procedure was responsible for 19.6% of 21.2% total error). We theorize this is due to our failure to grind or mill our samples to fine powder before digesting them in HCl. The importance of homogenizing soil samples prior to acid digestion with the goal of calculating IC content is well documented (e.g. Heron et al., 1997; Snyder & Trofymow, 2008; Walthert et al., 2010). We suggest soil samples be milled or ground before conducting acid digestion to derive IC content in order to reduce error by homogenizing each sample. Another procedural source of error arises at points where bulk density was estimated rather than measured. Most of the outliers at the high end of the dataset were points that had an estimated bulk density rather than calculated bulk density. In the future, we recommend utilizing more rigorous methods of extrapolating bulk density to depth than using the bulk density of the spatially closest sampling point.

Linear relationships between individual covariates and SOC stocks were examined to compare results to previous studies. The covariates that most strongly correlate with SOC stocks in our models at both sites are slope, NDVI MVC, soil clay content, and SWI. Previous studies have shown the relative efficacy of vegetation indices, slope, and SWI in predicting SOC stocks (Guo et al., 2020; Lacoste et al., 2014; Pouladi et al., 2019). Slope gradient has previously been shown to have a negative correlation with SOC stocks, and this relationship held true at both study sites (Guo et al., 2020; Kunkel et al., 2011; Lacoste et al., 2014). Vegetation indices have extensively been used as a predictor for SOC stocks because of the positive correlation between

primary productivity and SOC (Guo et al., 2020; Kunkel et al., 2011; Pouladi et al., 2019). NDVI was positively correlated with observed SOC stocks at the Alluvial Site and Regenerative Management Comparison Site, and negatively correlated with observed SOC stocks at the Conventional Management Comparison Site. Wetness indices such as SWI have been used extensively as a positive predictor for SOC stocks (Lacoste et al., 2014; Pouladi et al., 2019). SWI was positively correlated with SOC stocks at the Alluvial and Regenerative Management Comparison Sites, and negatively correlated with SOC stocks at the Conventional Management Comparison Site. I was unable to find any studies demonstrating the predictive power of USDA gSSURGO map unit soil clay content in digital soil mapping. This open source database of soil properties has the potential to be a powerful tool and merits additional utilization in future digital soil mapping endeavors. Clay content has been found to be one factor in predicting long-term carbon sequestration likely due to the mineral-associated SOC potential of clay (Torres-Sallan et al., 2017). Soil map unit clay content was positively correlated with SOC stocks at the Alluvial Site, and had no clear correlation with SOC stocks at either Management Comparison Site.

One particularly interesting deviation between the regenerative and conventional practices is the inverse relationship observed between NDVI MVC and SOC stocks at these sites. The alluvial site and the regenerative management comparison site display a positive relationship between NDVI MVC and SOC stocks, which has been previously documented (e.g. Duarte-Guardia et al., 2019; Kunkel et al., 2011). In contrast, the conventional site displays a weak negative relationship between SOC stocks and NDVI MVC. One possible explanation for this unexpected discrepancy is the feeding of hay during the winter. Crop residues applied to farmland have been shown to increase SOC stocks on a year-to-year basis (Blanchart et al., 2007; Chatterjee et al., 2018). Application of crop residue in the form of hay might lower the NDVI for

that portion of the field. The compounding effects of crop residue simultaneously increasing SOC stocks and decreasing the NDVI MVC values may be muddying the observed relationship at the conventional comparison site. Bale feeding was not employed at the Alluvial Site, partially explaining the better predictability of NDVI MVC.

## **Conclusion**

Although neither the RF or LM models were able to precisely predict SOC stocks at points, each model had a mean value of SOC stocks to 25 cm that is within  $\pm 1 \text{ Mg C ha}^{-1}$  of the observed values. Spatial variation in SOC stocks is either spatially too variable to model using RF and LM, or there are unmeasured covariates responsible for uncharacterized variation preventing models from making accurate point predictions. Among LM and RF, RF consistently provided stronger estimates of SOC stocks. We posit that RF is capable of satisfactorily estimating the mean SOC stocks to 25 cm of conventionally and regeneratively grazed pastures. However, more research is needed to verify this statement. We suggest further study that examines the minimum sample points required to make a reasonable estimation of mean SOC stocks using RF models. Additionally, the ability of a model to predict SOC stocks depends heavily on the landscape, historical management practices, and the relationships between individual covariates and SOC stocks.

## Appendix

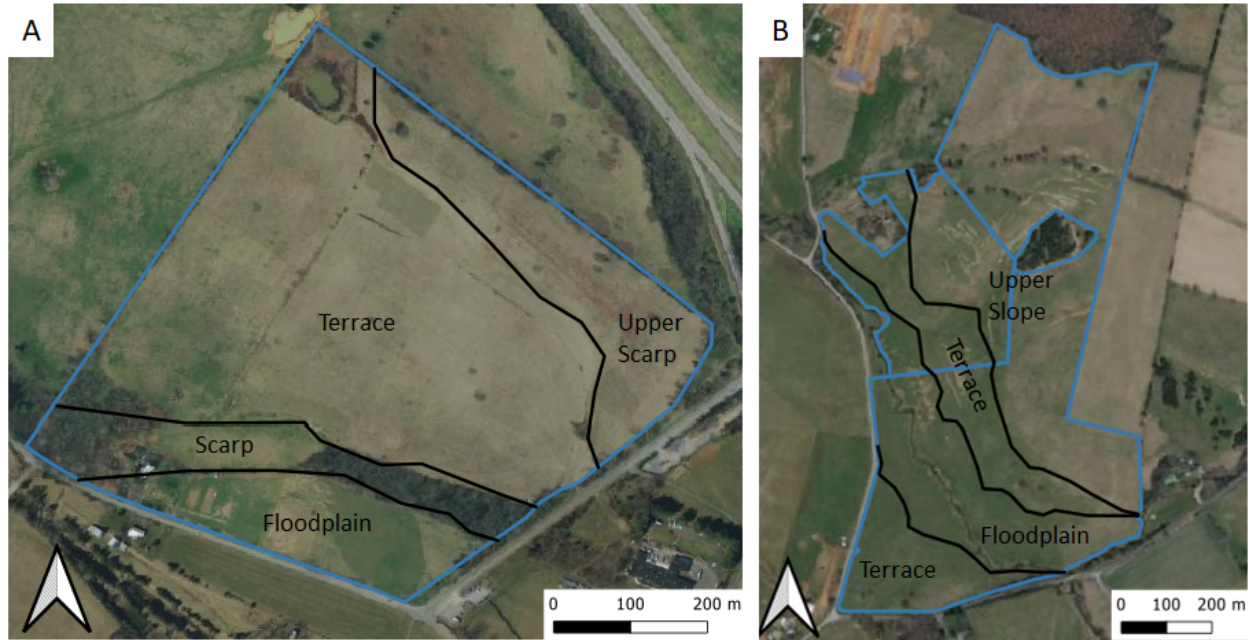


**Figure 1** - Map displaying Alluvial Site (A) and the Management Comparison Site (B) overlain with major geomorphic landforms at each site.

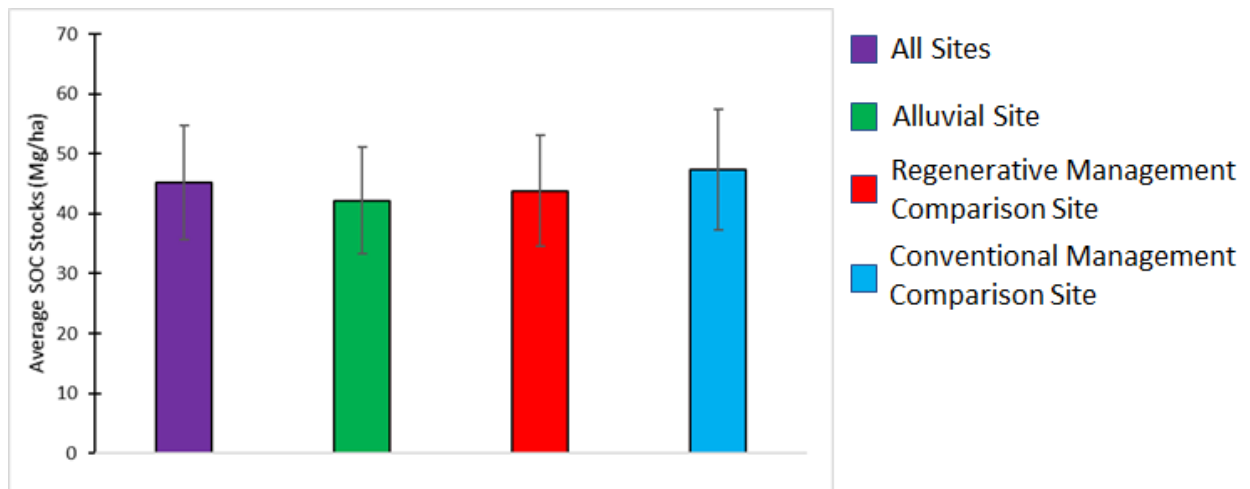


**Figure 2** - Average observed SOC stocks to 25 cm depth across all sites and individual sites with associated error.



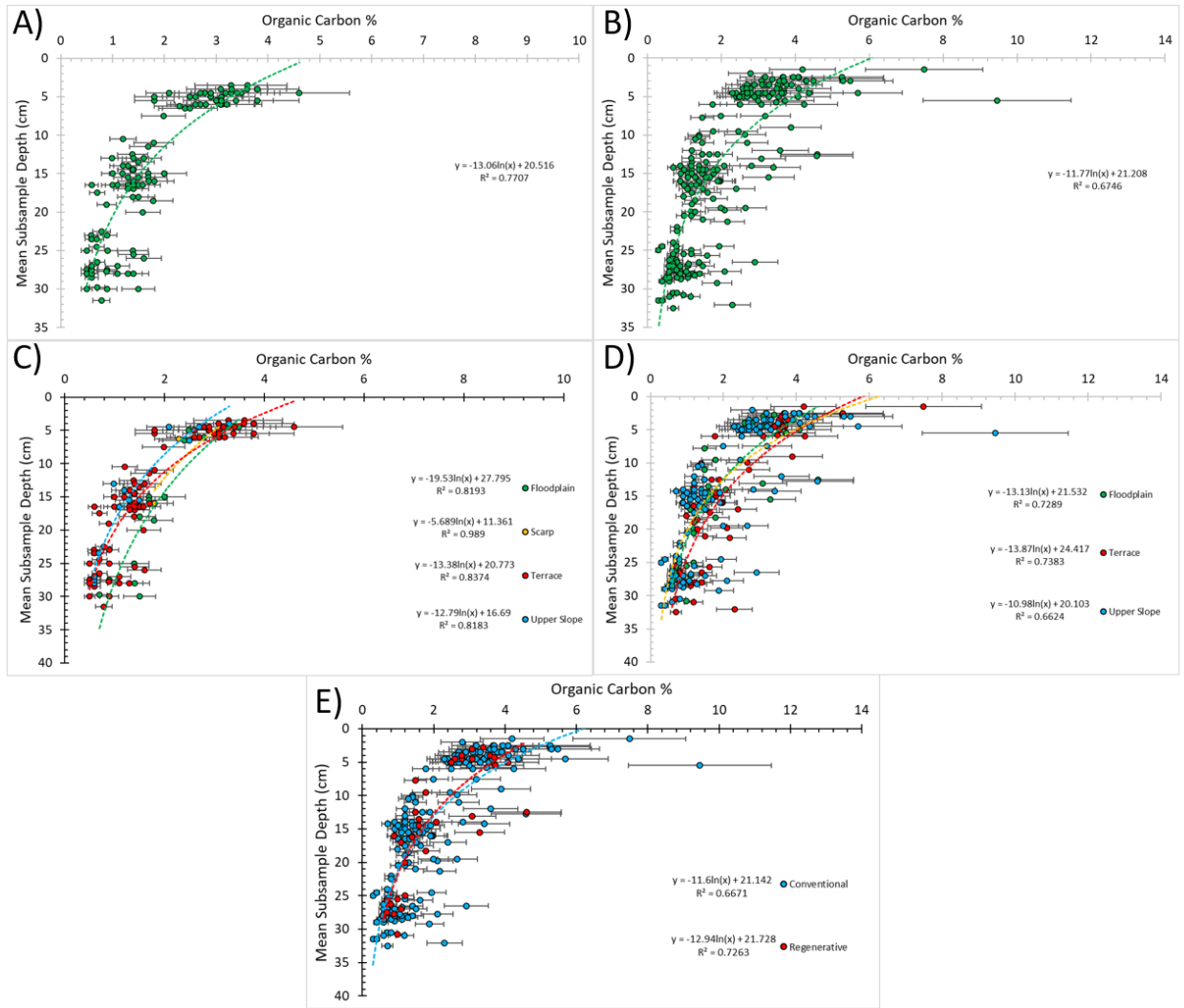


**Figure 3** - Percent organic carbon versus mean subsample depth for A) the Alluvial Site, B) the Management Comparison Site, C) geomorphic landforms at the Alluvial Site, D) geomorphic landforms at the Management Comparison Site, and E) by management type at the Management

Comparison site.

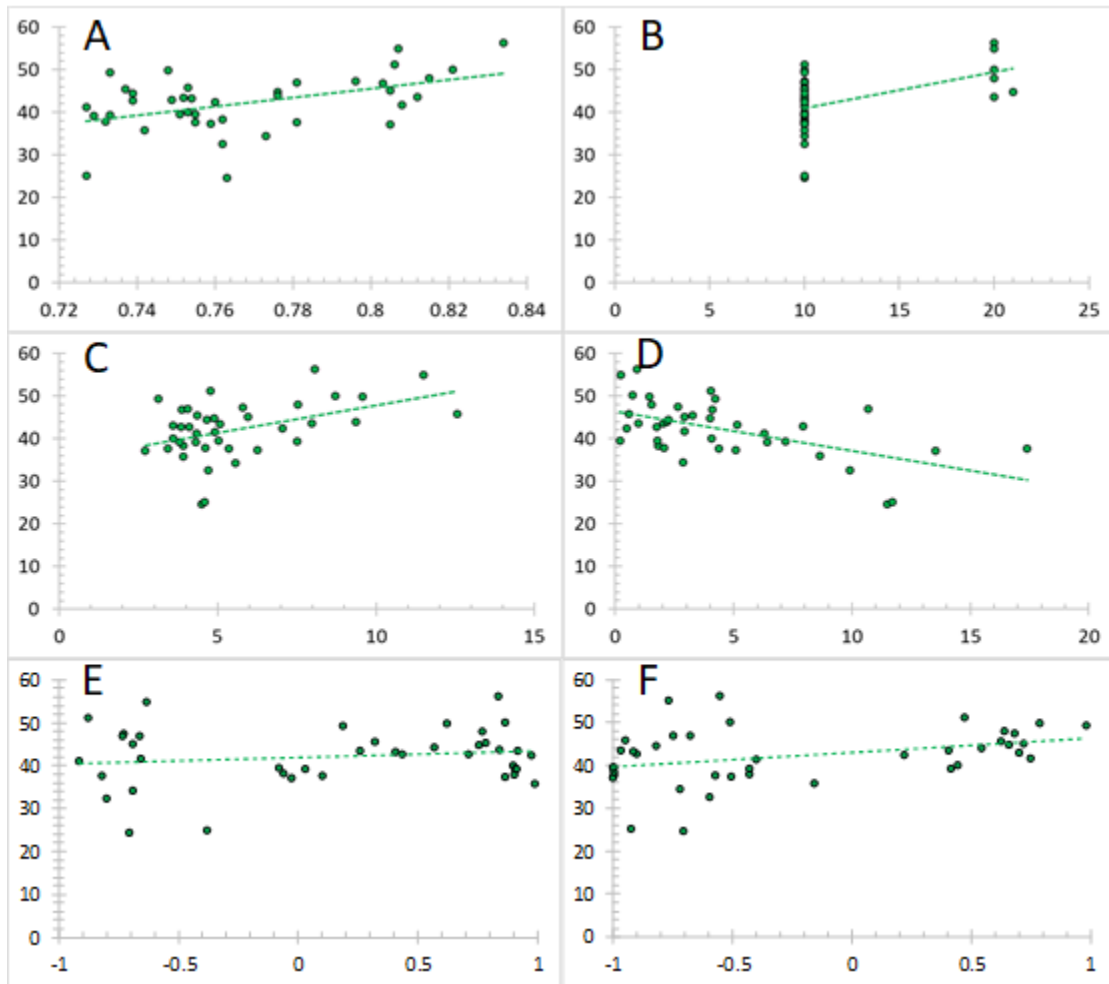


**Figure 4** - Single linear relationships between individual covariates on the x-axis and SOC stocks (Mg/ha) on the y-axis for the Alluvial Site. Individual Predictors are: A) NDVI MVC, B) Soil map unit clay content, C) SWI, D) Slope, E) Northness, and F) Eastness.  $R^2$  values are given in Table 1.

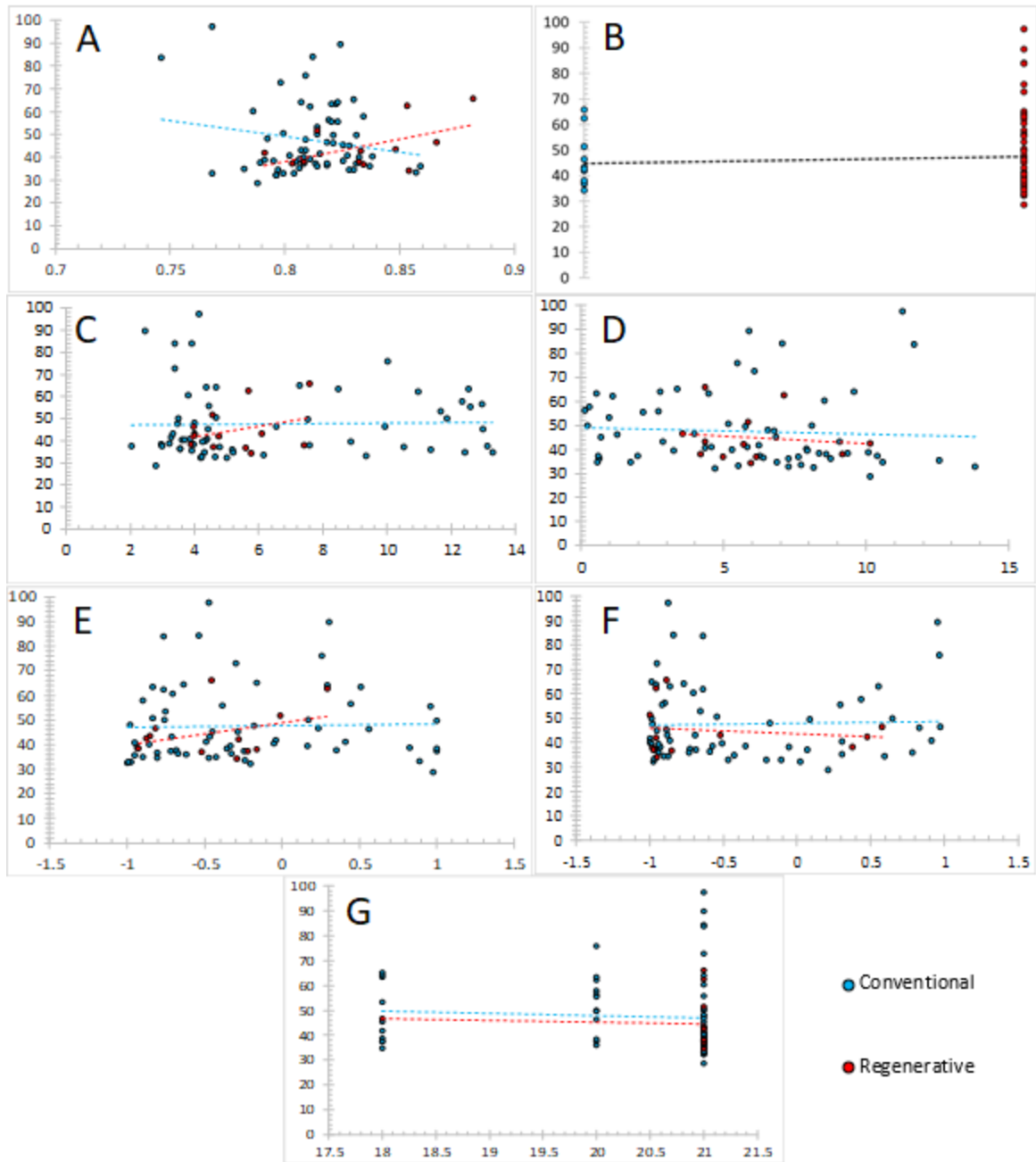


**Figure 5** - Single linear relationships between individual covariates on the x-axis and SOC stocks(Mg/ha) on the y-axis for the Management Comparison Site. Individual predictors are: A) NDVI MVC, B) Management Practices, C) SWI, D) Slope, E) Northness, F) Eastness, and G) Soil map unit clay content.  $R^2$  values are given in Table 1.



**Figure 6** - Rasters of Mg C ha<sup>-1</sup> SOC stocks to 25 cm at the Alluvial Site overlain with observed SOC stocks to 25 cm and geomorphic landforms. A) LM predicted raster. B) RF predicted raster.

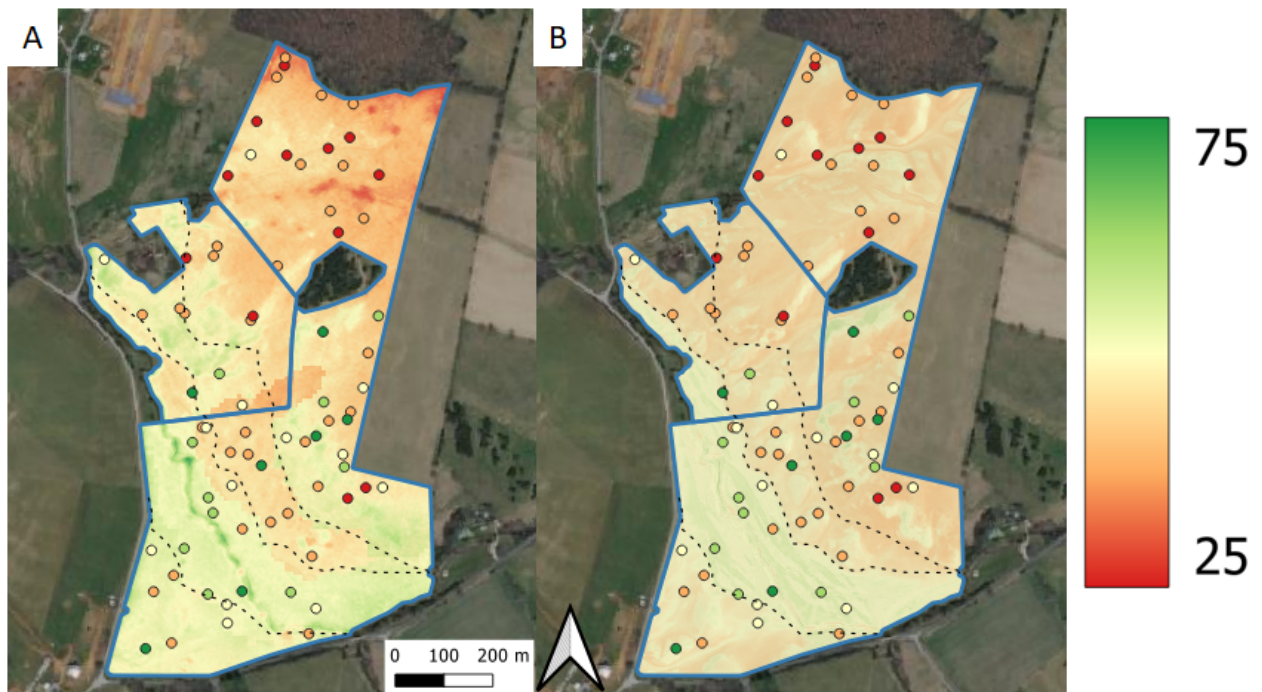


**Figure 7** - Rasters of Mg C ha<sup>-1</sup> SOC stocks to 25 cm at the Management Comparison Site overlain with observed SOC stocks to 25 cm and geomorphic landforms. A) LM predicted raster. B) RF predicted raster.

**Table 1** - R<sup>2</sup> values for each covariate derived by individual linear regressions.

Covariate	Alluvial Site	Regenerative Comparison	Conventional Comparison
NDVI MVC	0.22	0.25	0.03
Soil Clay Content	0.22	0.01	0.0002
SWI	0.19	0.15	0.01
Slope	0.32	0.09	0.01
Northness	0.02	0.09	0.01
Eastness	0.12	0.02	0.01
Management	N/A	0.005	0.005

**Table 2** - Observed and modelled SOC content to 25 cm in Mg C ha<sup>-1</sup>.

	Alluvial Site	Management Comparison Site
Observed	42.2 ± 8.9	46.8 ± 9.9
RF	41.9 ± 8.9	47.1 ± 10.0
LM	42.2 ± 8.9	46.8 ± 9.9

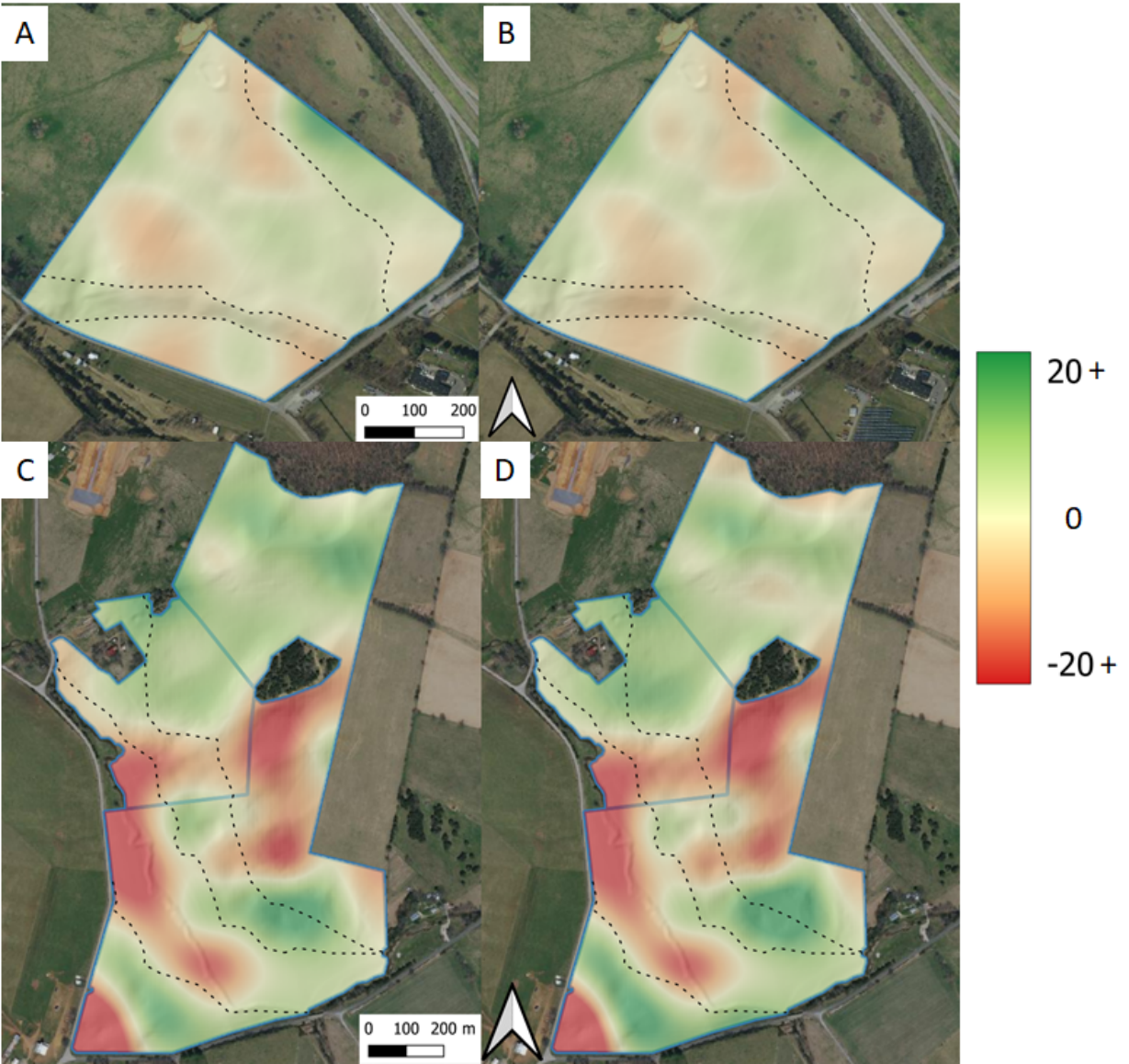


**Figure 8** - Surfaces interpolated via splines representing the SOC stock residuals derived from the: A) Alluvial Site RF, B) Alluvial Site LM, C) Management Comparison Site RF, and D) Management Comparison LM.

## References

- Allen, D. E., Pringle, M. J., Bray, S., Hall, T. J., O'Reagain, P. O., Phelps, D., ... & Dalal, R. C. (2014). What determines soil organic carbon stocks in the grazing lands of north-eastern Australia?. *Soil Research*, *51*(8), 695-706.
- Blanchart, E., Bernoux, M., Sarda, X., Siqueira Neto, M., Cerri, C. C., Piccolo, M., ... & Feller, C. (2007). Effect of direct seeding mulch-based systems on soil carbon storage and macrofauna in Central Brazil. *Agriculturae Conspectus Scientificus*, *72*(1), 81-87.
- Chan, K. Y., Oates, A., Li, G. D., Conyers, M. K., Prangnell, R. J., Poile, G., ... & Barchia, I. M. (2010). Soil carbon stocks under different pastures and pasture management in the higher rainfall areas of south-eastern Australia. *Soil Research*, *48*(1), 7-15.
- Chatterjee, S., Bandyopadhyay, K. K., Pradhan, S., Singh, R., & Datta, S. P. (2018). Effects of irrigation, crop residue mulch and nitrogen management in maize (*Zea mays* L.) on soil carbon pools in a sandy loam soil of Indo-gangetic plain region. *Catena*, *165*, 207-216.
- Conant, R. T., Cerri, C. E., Osborne, B. B., & Paustian, K. (2017). Grassland management impacts on soil carbon stocks: a new synthesis. *Ecological Applications*, *27*(2), 662-668.
- Conant, R. T., Six, J., & Paustian, K. (2003). Land use effects on soil carbon fractions in the southeastern United States. I. Management-intensive versus extensive grazing. *Biology and fertility of soils*, *38*(6), 386-392.
- Duarte-Guardia, S., Peri, P. L., Amelung, W., Sheil, D., Laffan, S. W., Borchard, N., ... & Ladd, B. (2019). Better estimates of soil carbon from geographical data: a revised global approach. *Mitigation and Adaptation Strategies for Global Change*, *24*(3), 355-372.
- Fonnesbeck, B. B., Boettinger, J. L., & Lawley, J. R. (2013). Improving a simple

- pressure-calculator method for inorganic carbon analysis. *Soil Science Society of America Journal*, 77(5), 1553-1562.
- Franzluebbers, A. J. (2010). Achieving soil organic carbon sequestration with conservation agricultural systems in the southeastern United States. *Soil Science Society of America Journal*, 74(2), 347-357.
- Follett, R. F., & Reed, D. A. (2010). Soil carbon sequestration in grazing lands: societal benefits and policy implications. *Rangeland Ecology & Management*, 63(1), 4-15.
- Guo, L., Fu, P., Shi, T., Chen, Y., Zhang, H., Meng, R., & Wang, S. (2020). Mapping field-scale soil organic carbon with unmanned aircraft system-acquired time series multispectral images. *Soil and Tillage Research*, 196, 104477.
- Heron, G., Barcelona, M. J., Andersen, M. L., & Christensen, T. H. (1997). Determination of nonvolatile organic carbon in aquifer solids after carbonate removal by sulfurous acid. *Groundwater*, 35(1), 6-11.
- Kane, D., Oldfield, E., & Bradford, M. (2019). Quick Carbon: A Rapid, Landscape-Scale Soil Carbon Assessment Tool. AGU Fall Meeting 2019. Digital Poster.
- Kunkel, M. L., Flores, A. N., Smith, T. J., McNamara, J. P., & Benner, S. G. (2011). A simplified approach for estimating soil carbon and nitrogen stocks in semi-arid complex terrain. *Geoderma*, 165(1), 1-11.
- Lacoste, M., Minasny, B., McBratney, A., Michot, D., Viaud, V., & Walter, C. (2014). High resolution 3D mapping of soil organic carbon in a heterogeneous agricultural landscape. *Geoderma*, 213, 296-311.
- Lagacherie, P. (2008). Digital soil mapping: a state of the art. *Digital soil mapping with limited data*, 3-14.



- Malone, B. P., McBratney, A. B., Minasny, B., & Laslett, G. M. (2009). Mapping continuous depth functions of soil carbon storage and available water capacity. *Geoderma*, *154*(1-2), 138-152.
- McBratney, A. B., Santos, M. M., & Minasny, B. (2003). On digital soil mapping. *Geoderma*, *117*(1-2), 3-52.
- Minasny, B., & McBratney, A. B. (2006). A conditioned Latin hypercube method for sampling in the presence of ancillary information. *Computers & geosciences*, *32*(9), 1378-1388.
- Mosier, S., Apfelbaum, S., Byck, P., Calderon, F., Teague, R., Thompson, R., & Cotrufo, M. F. (2021). Adaptive multi-paddock grazing enhances soil carbon and nitrogen stocks and stabilization through mineral association in southeastern US grazing lands. *Journal of Environmental Management*, *288*, 112409.
- Planet Team (2020). Planet Application Program Interface: In Space for Life on Earth. San Francisco, CA. <https://api.planet.com>.
- Pouladi, N., Møller, A. B., Tabatabai, S., & Greve, M. H. (2019). Mapping soil organic matter contents at field level with Cubist, Random Forest and kriging. *Geoderma*, *342*, 85-92.
- Sanderman, J., Reseigh, J., Wurst, M., Young, M. A., & Austin, J. (2015). Impacts of rotational grazing on soil carbon in native grass-based pastures in southern Australia. *PLoS One*, *10*(8), e0136157.
- Schrumpf, M., Schulze, E. D., Kaiser, K., & Schumacher, J. (2011). How accurately can soil organic carbon stocks and stock changes be quantified by soil inventories?. *Biogeosciences*, *8*(5), 1193-1212.
- Singh, K., Murphy, B. W., & Marchant, B. P. (2013). Towards cost-effective estimation of soil carbon stocks at the field scale. *Soil Research*, *50*(8), 672-684.

Snyder, J. D., & Trofymow, J. A. (1984). A rapid accurate wet oxidation diffusion procedure for determining organic and inorganic carbon in plant and soil samples. *Communications in Soil Science and Plant Analysis*, 15(5), 587-597.

Soil Survey Staff. The Gridded Soil Survey Geographic (gSSURGO) Database for Virginia. *United States Department of Agriculture, Natural Resources Conservation Service*. Available online at <https://gdg.sc.egov.usda.gov/>. June 16, 2020 (201909 official release).

Torres-Sallan, G., Schulte, R. P., Lanigan, G. J., Byrne, K. A., Reidy, B., Simó, I., ... & Creamer, R. E. (2017). Clay illuviation provides a long-term sink for C sequestration in subsoils. *Scientific Reports*, 7(1), 1-7.

Virginia Department of Mines, Minerals, and Energy. (2020). 1 m DEM from 3DEP LiDAR Survey. Retrieved February 2020 from <https://www.usgs.gov/core-science-systems/ngp/tnm-delivery>

Walthert, L., Graf, U., Kammer, A., Luster, J., Pezzotta, D., Zimmermann, S., & Hagedorn, F. (2010). Determination of organic and inorganic carbon,  $\delta^{13}\text{C}$ , and nitrogen in soils containing carbonates after acid fumigation with HCl. *Journal of Plant Nutrition and Soil Science*, 173(2), 207-216.

Web Soil Survey. (2019). Retrieved March 15, 2021, from <https://websoilsurvey.sc.egov.usda.gov/App/WebSoilSurvey.aspx>

Wilkes, G. P., Spencer, E. W., Evans, N. H., & Campbell, E. V. M. (2007). Geology of Rockbridge County, Virginia (Publication 170) (p. 31). Charlottesville, Va.: Commonwealth of Virginia, Dept. of Mines, Minerals and Energy, Division of Mineral Resources.

Yang, Y. Y., Goldsmith, A., Herold, I., Lecha, S., & Toor, G. S. (2020). Assessing Soil Organic

Carbon in Soils to Enhance and Track Future Carbon Stocks. *Agronomy*, 10(8), 1139.

Zhang, Y., Ji, W., Saurette, D. D., Easher, T. H., Li, H., Shi, Z., ... & Biswas, A. (2020).

Three-dimensional digital soil mapping of multiple soil properties at a field-scale using regression kriging. *Geoderma*, 366, 114253.